A Fully-Embedded Two-Stage Coder for Hyperspectral Near-lossless Compression

Jente Beerten, Ian Blanes, *Member, IEEE,* and Joan Serra-Sagristà, *Senior Member, IEEE*

***Abstract*—This letter proposes a near-lossless coder for hyperspectral images. The coding technique is fully embedded and minimizes the distortion in the l_2 norm initially and in the l_∞ norm subsequently. Based on a two-stage near-lossless compression scheme, it includes a lossy and a near-lossless layer. The novelties are: the observation of the convergence of the entropy of the residuals in the original domain and in the spectral-spatial transformed domain; and an embedded near-lossless layer. These contributions enable a progressive transmission while optimising both SNR and PAE performance. The embeddedness is accomplished by bitplane encoding plus arithmetic encoding. Experimental results suggest that the proposed method yields a highly competitive coding performance for hyperspectral images, outperforming multi-component JPEG2000 for l_∞ norm and pairing its performance for l_2 norm, and also outperforming M-CALIC in the near-lossless case –for PAE $\geq$ 5–.**

I. Introduction

REMOTE sensing images are becoming more important in modern society. These images tend to be very large and there is an increasing need for high performing image compression techniques. A desired characteristic of such compression techniques is that the image can be progressively refined while transmitting the bitstream, which asks for an embedded coder (i.e., one that by truncating a compressed file can select a desired compression level). This is an interesting feature for remote sensing images because transmitting them completely can consume a considerable amount of time, and consumers may want to obtain first an image at a certain quality level and subsequently decide if higher quality versions are desired.

Typically, image compression techniques are classified into three modalities: lossless, lossy and near-lossless. Lossless compression allows to reconstruct the original image perfectly. The obtained compression ratio is rather low because a perfect reconstruction is demanded. Lossy compression approximates the original image I, while typically minimising the distortion in the l_2 norm. Allowing a certain distortion in the reconstructed image $\hat{I}$ leads to a higher compression performance. Near-lossless compression was introduced for applications that require a tight bound in the l_∞ norm, like remote sensing [1] or medical imaging [2], where a large error in a pixel could potentially induce a wrong classification or diagnosis. Near-lossless techniques bound the l_∞ norm —also known as peak absolute error (PAE) or Maximum Absolute Distortion (MAD)— so that it is limited to a certain tolerance value. We refer to this tolerance value as δ:

$$\|I - \hat{I}\|_\infty = \max |I_{x,y,z} - \hat{I}_{x,y,z}| \leq \delta \quad (1)$$

Our proposed technique is a near-lossless coder. When δ=0, it becomes a pure lossless compression technique. The technique produces a fully embedded codestream and minimises the distortion in the l_2 norm initially and in the l_∞ norm subsequently. The proposal belongs to the class of two-stage coders, i.e., a lossy layer followed by a near-lossless layer. The lossy layer approximates the original image. Then the residual is calculated by subtracting the approximated image from the original image. The near-lossless layer quantizes the residual so that PAE $\leq \delta$ and encodes the result losslessly. The problem with such a two-stage coder is that the compression performance is dependent on how much distortion is introduced in the lossy layer, or equivalently on how much *lossy bit rate* is allocated. Our proposal uses the approach introduced in [3] to determine the amount of lossy bit rate. JPEG2000 [4], a fully-embedded technique, is used for the lossy layer, while bitplane encoding (BPE) plus arithmetic encoding form an embedded near-lossless layer, yielding the first fully embedded two-stage coder. Furthermore, our proposal provides competitive performance for remote sensing images because it successfully incorporates a spectral transform.

This paper is organised as follows: section II provides a literature review of near-lossless compression methods. Section III describes our proposal. Section IV presents experimental results and Section V concludes.

II. Literature overview

Most near-lossless compression techniques can be classified into, again, three categories, depending on how near-lossless is provided: based on predictive coding, based on prequantization followed by lossless coding, or based on two-stage near-lossless coders.

The first near-lossless compression category builds upon predictive coding [5], [6], [7], [8]. Techniques in this category scan the image in a certain fixed order and make a prediction of the current pixel value based on previously encoded pixels (causal context). The difference between the predicted and the original pixel is called the prediction error. Only this prediction error is encoded. A near-lossless compression scheme is obtained by applying a scalar quantization on these prediction errors. The two most popular predictive techniques are CALIC [5] and JPEG-LS [6], [9]. Although CALIC has a higher computational complexity, since its compression performance is usually superior, it is often used as a benchmark near-lossless coding technique. The drawback of these two predictive coding techniques is that they do not offer any

This work was supported in part by FEDER, the Spanish Government (MINECO), and the Catalan Government, under grants TIN2012-38102-C03-03 and 2014SGR-691.

The authors are with the Department of Information and Communications Engineering, Universitat Autònoma de Barcelona, Cerdanyola del Vallès, 08193 Barcelona, Spain (e-mail: jente.beerten@deic.uab.cat; ian.blanes@uab.cat; joan.serra@uab.cat).

Post-print of: Beerten, J., Blanes, I. and Serra Sagristà, J. "A fully embedded two-stage coder for hyperspectral near-lossless compression" in IEEE geoscience and remote senning letters, vol. 12, no. 8 (August 2015), p. 1775-1779. DOI 10.1109/LGRS.2015.2425548
Cop. 2015. IEEE. Personal use of this material is permitted. Permissions from IEEE must be obtained for all other uses, in any current or future media, including reprinting/republishing this material for advertising or promotional purposes, creating new collective works, for resale or redistribution to servers or lists, or reuse of any copyrighted component of this work in other Works.

degree of embedding. Furthermore, predictive techniques are not able to capture global patterns because they work locally in the image. Thus, quality of the predictions deteriorates for larger values of δ and, consequently, their compression performance diminishes [10]. To increase the compression performance in the l_2 norm sense at the expense of a worse distortion in the l_∞ norm, a technique [11] was introduced, where the image is first compressed with CALIC and then soft-decoding is applied on the recovered image. Also, to exploit the spectral correlation in hyperspectral images, 3D-CALIC [12] and M-CALIC [13] were proposed. While 3D-CALIC uses both an intra-band and an inter-band predictor, M-CALIC uses only an inter-band predictor. Recently, [14] described a novel rate control algorithm for onboard predictive coding that allows near-lossless coding and rate control.

The second near-lossless compression category builds upon first prequantizing the pixels with a scalar quantizer, and then employing a lossless compression technique. This approach is known to yield poor performance for large values of δ [10]. In [15], [16] such a near-lossless compression scheme is implemented based on an extension of CCSDS-IDC [17] for satellite images; instead of a scalar quantization, a quantization table is used to increase the PSNR performance.

The third near-lossless compression category builds upon pairing a lossy and a lossless compression technique. A lossy approximation is first produced by a lossy coding technique, and then the residual (i.e., the difference between the original image and the approximated image), is quantized and losslessly encoded. Different two-stage proposals have appeared in the literature. The first proposal [18] employed a wavelet based approach (SPIHT [19]) as the lossy layer and encoded the residual through CALIC. A similar proposal was presented in [10], with a modified version of CALIC. These two proposals have a certain degree of embedding thanks to the lossy layer. However, one drawback is that their performance also depends on the bit rate of the lossy layer; in these two proposals, the optimal lossy bit rate has to be determined by iteration. Next, [20] proposed to use a lossy layer with a fixed lossy bit rate plus an embedded near-lossless quantization layer. The near-lossless layer consists of entropy encoding and context modelling. This proposal is limited in that only a selective number of values of δ are possible. Finally, a solution for determining the optimal lossy bit rate was proposed in [3]. The optimal lossy bit rate is determined by estimating the entropy of the wavelet residual, as it converges to the quantized pixel-domain residual when the lossy bit rate increases. This approach avoids the need for a computationally demanding iteration to determine the optimal bit rate or the use of complex context modeling. Later, l_∞-error scalability was introduced to this method [21]. More recently, [22] presented a two-stage coder with JPEG2000 as the lossy layer and 2D-CALIC as the lossless layer; here, the optimal lossy bit rate is not optimized and the lossless layer is not embedded. Lastly, [23] proposed a near-lossless compression scheme for satellite images, where the lossy layer consists of CCSDS-IDC [24] and the residual is encoded with BPE; however, this technique does not determine an optimal lossy bit rate either.

There are three other techniques worth mentioning that do not fall into the above near-lossless categories. In [25] and [26], a near-lossless compression proposal is introduced by refining pixel intervals, yielding a progressive –but not embedded– codestream. In [27], deadzone quantization was incorporated.

III. Proposal

The proposed technique belongs to the class of two-stage coders. The lossy layer can consist of any lossy embedded compression method such as SPIHT, JPEG2000, CCSDS-IDC or TCE [28]. In our compression proposal we have incorporated JPEG2000 as the lossy layer. The near-lossless layer consists of bitplane encoding and arithmetic encoding. We employ [3] to estimate the optimal lossy bit rate and then arithmetically encode the pixel-domain residual in a bitplane-by-bitplane fashion, yielding a fully embedded codestream.

A. Convergence of the entropy of the residuals

In [3] a method was introduced to find the optimal lossy bit rate. It was shown that the entropy of the residual in the wavelet domain $H(Y)$ and in the original (pixel) domain $H(X)$ starts to coincide after the critical lossy bit rate R_c (assuming an order-zero source for the purposes of entropy calculations). Above this critical bit rate, the residual lacks the good structure that a good lossy encoder can take advantage of. In addition, the coding performance is as good and usually worse than employing an arithmetic encoder. Because of this property the optimal lossy bit rate can be found when the sum of the lossy bit rate and the entropy of the residual in the wavelet domain attain a minimum. This approach avoids the need to iteratively apply the inverse wavelet transform to find the optimal lossy bit rate.

However, when coding hyperspectral images, a spectral transform is needed to account for the spectral correlation of hyperspectral images, usually larger than the spatial correlation. It has been reported that the KLT provides one of the highest coding performances [28], [29], [30]. In our proposal, we thus include a KLT prior to the lossy layer and show that the optimal lossy bit rate can still be found (at the receiver, the KLT is inverted right after the lossy layer decoding). Fig. 1 presents our proposed two-stage encoder: the original image I goes first through a spectral transform and then through a wavelet-based coder, yielding an embedded codestream I''. Still at the encoder, the decoding of this codestream is also carried out, so as to obtain a recovered image I' that is then subtracted from the original image I to generate a residual or error image e. This residual image is then fed into a quantization step and later into an entropy coding step, producing a second codestream e''. At the decoder side, codestreams I'' and e'' have to be decoded, and the produced signals are combined to produce a single recovered image. In our proposal, we have incorporated the KLT as a spectral transform step and codestream e'' is also embedded. We note that the KLT is likely to be the most expensive operation of the whole encoding process, regardless of the particular lossy method, and not having to iteratively invert it to find the optimal lossy bit rate is a quasi-mandatory requirement.

We now report the convergence of the entropy of the residual also in the spectrally-transformed domain $H(Z)$.

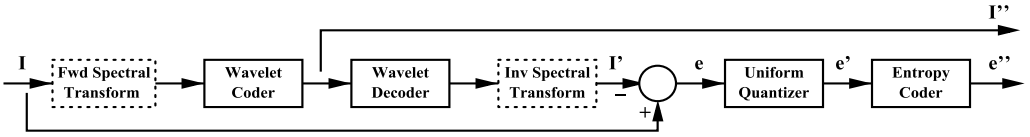

Fig. 1: Diagram of a two-stage encoder. Our proposal incorporates a spectral transform to account for the spectral correlation.

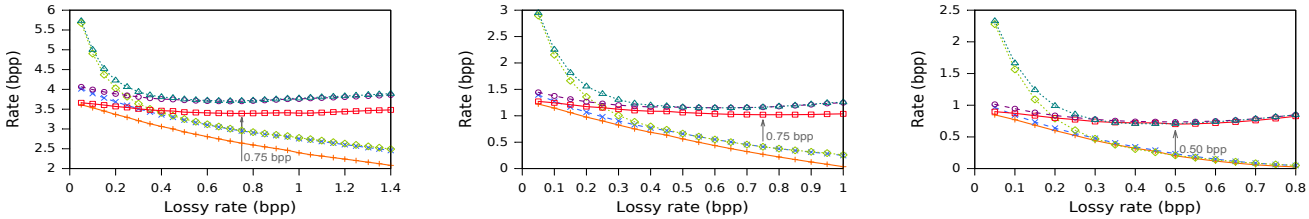

(a) $\delta = 0$; lossy rate is 0.75 bpp. (b) $\delta = 3$; lossy rate is 0.75 bpp. (c) $\delta = 5$; lossy rate is 0.50 bpp.

Fig. 2: Convergence of the residual entropies for Yellowstone Radiance image in three different domains (original ···◇···, spectral – × –, and spectral-spatial —+—) and total rate corresponding to the residual entropy plus the bit rate needed for the lossy layer (original ···△···, spectral – ⊖ –, and spectral-spatial —□—).

Namely, we consider the original domain $H(X)$, the spectral domain $H(Z)$ and the spectral-spatial domain $H(Y)$ (2D wavelet transform is applied after 1D spectral transform). A static binary arithmetic encoder is employed in our proposal, meaning that the exact frequencies are fed to the encoder. There are scenarios where implementation issues may hinder the performance of arithmetic encoders, such as when large frequency tables need be transmitted, or when the precision of frequencies is not high enough; nonetheless, in this case, the cost of transmitting these frequencies is negligible with respect to the large size of hyperspectral images and their precision can be as high as needed. This implies that the entropy of the residual in the original domain can be considered equal to the real bit rate. Fig. 2 shows the entropy of the residuals (residual rate) and the total bit rate, for each domain, for AVIRIS Yellowstone Radiance image for $\delta = 0$, $\delta = 3$ and $\delta = 5$. Although there is a certain offset between the entropies in the different domains, our proposal is able to find the optimal lossy bit rate accurately also after incorporating the spectral transform. For a given image, the residual entropy is in coarse terms a decreasing monotonic function the lossy rate, as is the optimum lossy bitrate, in coarse terms, a decreasing monotonic function of delta. Nonetheless, it is also possible to use a larger, and perhaps more advantageous, lossy layer at the expense of a slight increase in the total bit rate for $\delta = 0$ and $\delta = 3$, as can be seen in Fig. 2.

B. Near-lossless embedded stage

The residual signal is encoded through a custom context-less BPE because it enables an embedded codestream, and also because PAE decreases substantially after each transmitted bitplane. Within the BPE, each bitplane is encoded with a binary arithmetic encoder. More specifically, each bit plane of each component is encoded separately to ensure that the encoding can be stopped at any arbitrary bit rate. The pixel-domain residual has a symmetric probability mass function (pmf) with zero as the expected value. This means that bitplane encoding can be achieved by mapping the integer values to natural values. This mapping was also used in [31] to entropy encode symmetrically distributed image values. The mapping consists of reordering an ordered sequence of values to 0, 1, -1, 2, -2, ... This will then lead to a decaying single-sided pmf. In the end we thus have a one-to-one mapping of integer to natural values. The described mapping is shown in Equation 2. Note that the reordering is done after the quantization of the pixel-domain residual with the appropriate δ. After the mapping the natural values are transformed to their binary representation. The last bit in the binary representation corresponds to a sign bit. This sign bit is sent immediately after the first significant bit of a residual coefficient is sent (i.e., when a magnitude bitplane contains a one). A significance matrix keeps track of all the sign bits that have been sent.

$$f(x) = \begin{cases} 2|x| - 1, & \text{if } x > 0 \\ 2|x|, & \text{if } x \leq 0 \end{cases}. \tag{2}$$

IV. Experimental results

This section investigates the coding performance of the proposed fully embedded near-lossless coder. First, performance in terms of bit rate is assessed through comparison to other near-lossless/lossless coders. Second, SNR and PAE performance are analyzed. Performance is evaluated over a set of AVIRIS [32] and Hyperion [33] hyperspectral images, publicly available for download. Technical names and sizes are provided in Table I, along with the entropy of the images and that of the quantized versions of the images. All images are 16 bits per pixel per band (bpppb), except for Hawaii and Maine that are 12 bpppb. Uncalibrated images are stored as unsigned integers, whereas calibrated images are stored as signed integers. Hyperion calibrated images are radiance images.

A. Lossless and Near-lossless compression performance

The proposed method is compared against three state-of-the-art coding techniques: M-CALIC [13], [35] and CCSDS-123.0-B-1 with a quantizer [14], examples of near-lossless techniques based on predictive coding; and against "Prequantization+MC-JPEG2000", which simulates proposal [10], an example of near-lossless technique based on prequantization.

M-CALIC performs an inter-band prediction in BSQ mode (with negative values on the first row of Hyperion images set

TABLE I: AVIRIS and Hyperion images used in the experiments.Technical names, size and entropy of original and prequantized versions for different δ values are provided.

Sensor	Name	Acronym	Technical Name	Size ($x \times y \times z$)	Entropy				
					δ=0	δ=1	δ=5	δ=32	δ=128
AVIRIS	Hawaii Uncalibrated	H	f011020t01p03r05_sc01	614 × 512 × 224	8.55	6.99	5.14	2.79	1.16
	Maine Uncalibrated	M	f030828t01p00r05_sc10	680 × 512 × 224	9.09	7.52	5.70	3.34	1.76
	Yellowstone Radiance	YR	f060925t01p00r12_sc00	677 × 512 × 224	10.33	8.75	6.92	4.49	2.71
	Yellowstone Uncalibrated	YU	f060925t01p00r12_sc00	680 × 512 × 224	12.62	11.04	9.16	6.63	4.71
Hyperion	Agricultural Calibrated	A	EO1H0280342004074110PX	256 × 3129 × 242	10.05	8.74	7.16	4.95	3.32
	Coral Reef Calibrated	C	EO1H0830742003120110PW	256 × 3127 × 242	8.46	7.11	5.44	3.22	1.93
	Urban Calibrated	U	EO1H0440342002212110PY	256 × 3176 × 242	10.01	8.70	7.10	4.85	3.24
	Erta Ale Uncalibrated	E	EO1H1680502010057110KF	256 × 3242 × 242	9.46	7.88	6.03	3.54	1.76
	Lake Monona Uncalibrated	L	EO1H0240302009166110PF	256 × 3352 × 242	9.91	8.33	6.47	3.97	2.18

TABLE II: Comparison of different near-lossless for several values of δ. Coding performance is reported in bits per pixel per band. Bold font indicates highest coding performance. Results for CCSDS-123.0 + Quantizer are from [34].

Img	M-CALIC					CCSDS-123.0 + Quantizer					Preq. + MC-JPEG2000					Proposal				
δ	*0*	*1*	*5*	*32*	*128*	*0*	*1*	*5*	*32*	*128*	*0*	*1*	*5*	*32*	*128*	*0*	*1*	*5*	*32*	*128*
H	2.84	1.57	0.65	0.20	0.10	2.63	1.39	0.40	—	—	2.89	2.28	2.06	1.57	0.54	**2.45**	**1.01**	**0.18**	**0.07**	**0.07**
M	2.89	1.62	0.69	0.23	0.12	2.72	1.46	0.45	—	—	3.02	2.40	2.20	1.96	1.55	**2.62**	**1.16**	**0.23**	**0.07**	**0.07**
YR	4.13	2.64	1.28	0.39	0.16	—	—	—	—	—	3.90	2.89	2.38	2.16	1.91	**3.76**	**2.24**	**0.70**	**0.18**	**0.07**
YU	6.32	4.73	2.91	1.03	0.41	6.20	4.59	2.77	—	—	6.11	4.52	3.07	2.46	2.24	**5.96**	**4.37**	**2.54**	**0.53**	**0.23**
A	**5.29**	**4.05**	**2.61**	0.99	0.34	5.32	4.01	3.43	—	—	5.79	4.44	3.11	2.16	1.91	6.12	4.53	2.78	**0.84**	**0.18**
C	**4.62**	**3.47**	**2.09**	0.70	0.30	4.94	3.63	3.09	—	—	5.41	4.13	2.86	1.96	1.70	5.81	4.22	2.41	**0.61**	**0.12**
U	**5.15**	**3.97**	**2.54**	0.99	0.39	5.31	4.01	3.42	—	—	5.79	4.44	3.15	2.20	1.92	6.14	4.56	2.81	**0.89**	**0.23**
E	4.75	3.19	1.59	0.28	0.07	4.61	3.09	2.42	—	—	**4.46**	3.19	2.51	2.14	1.61	4.55	**3.00**	**1.26**	**0.12**	**0.06**
L	4.93	3.35	1.72	0.34	0.07	4.69	3.17	2.49	—	—	**4.60**	3.30	2.53	2.13	1.69	4.65	**3.09**	**1.38**	**0.17**	**0.06**

to 0). "Prequantization+MC-JPEG2000" performs a spectral Reversible KLT [36] and JPEG2000 (BOI) with a reversible 5/3 spatial wavelet transform with 5 levels. Our proposal performs a KLT spectral transform and JPEG2000 (BOI) with an irreversible 9/7 spatial wavelet transform with 5 levels; encoding of the residual is implemented in java with an arithmetic encoder derived from the MQ coder of JPEG2000.

Table II reports results in terms of bit rate. Results for prediction-based techniques illustrate how the bit rate decreases quickly as a function of δ. The prequantization-based technique leads to good results for $\delta = 0$, but its performance deteriorates for larger values of δ. For AVIRIS images, our proposal yields always the best performance. For Hyperion uncalibrated images, the prequantization-based technique beats our proposal by a negligible margin only for $\delta = 0$. For Hyperion calibrated images, M-CALIC proves superior by 13% for $\delta \leq 5$; however, M-CALIC doesn't offer any degree of embedding, while the proposed method offers a fully embedded codestream; for $\delta > 5$, our proposal is the most competitive.

B. Embedded SNR performance

In order to study the rate-distortion performance in terms of SNR (l_2 norm), we compare our proposal against another approach that also provides fully embedded codestreams and that has been optimized minimizing the l_2 norm, namely, Prequantization+MC-JPEG2000. Results for CCSDS-123 with Quantizer are not included in this section, as those available in [14] are only for on-board operation (employing a heavily constrained rate control method). Other near-lossless coding techniques do not provide either an embedded codestream or a competitive performance and are thus not compared here.

Fig. 3 reports results for three images and two different δ values. Reporting results for larger values of δ would show the poor performance of the prequantization-based technique (these results are not reported due to space constraints). On most occasions, our two-stage proposed method has the same SNR performance as MC-JPEG2000 until the lossy bit rate (for example, in (b) optimal lossy bit rate is 0.6 bpp for $\delta = 0$ and for $\delta = 1$; note that these values of δ determine the maximum bit rate as well). At some point the errors introduced in the reversible lifting network of the RKLT start dragging down the performance of the prequantization-base method. This is very noticeable for the Hawaii image and increases with larger δ values. In general and in addition to its near-lossless capabilities, the proposed technique provides better progressive SNR performance while achieving similar lossless results; it is thus a good candidate to replace the use of a RKLT+JPEG2000 approach to supply progressive lossy-to-lossless compression.

C. Embedded PAE performance

To conclude the analysis of the rate-distortion performance, the PAE metric (l_∞ norm) is investigated. Fig. 4 reports results for, again, three images and two different δ values. We see that the PAE of the proposed method decreases significantly, and in flat steps, after the optimal lossy bit rate (for both $\delta = 0$ and $\delta = 1$), as it enters near-lossless operation mode. On the other hand, PAE decreases in a non-constant manner for the other embedded coding technique.

V. Conclusion

A two-stage near-lossless coding technique providing a fully embedded codestream has been proposed. The two-stage coder consists of a lossy layer (usually already providing embedded codestreams) and a near-lossless layer. Our proposal introduces embeddedness in the near-lossless layer through mapping, bitplane-by-bitplane processing and arithmetic encoding. In addition, a spectral transform was included to account for the spectral correlation among components in hyperspectral images. Experimental results indicate that the proposed technique yields a competitive coding performance for lossless compression, and the best coding performance for near-lossless compression for $\delta \geq 5$. Moreover, thanks

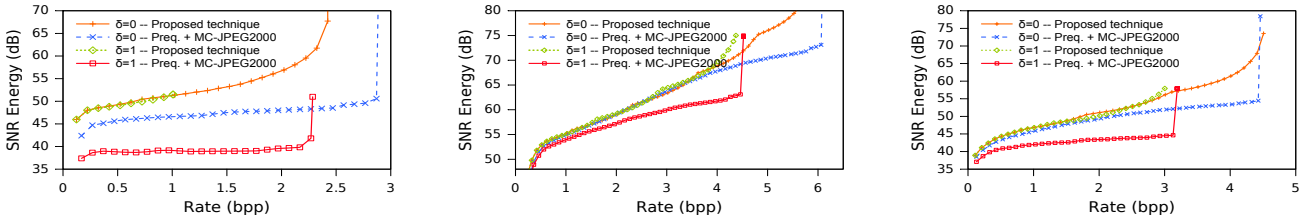

(a) Hawaii (b) Yellowstone Uncalibrated (c) Erta Ale

Fig. 3: SNR performance of the proposed method for $\delta = 0$ and $\delta = 1$ as compared to Prequantization+JPEG2000.

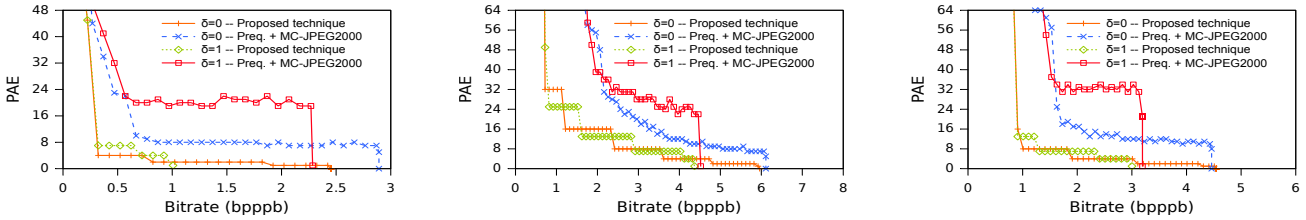

(a) Hawaii (b) Yellowstone Uncalibrated (c) Erta Ale

Fig. 4: PAE performance of the proposed method for $\delta = 0$ and $\delta = 1$ as compared to Prequantization+JPEG2000.

to its lossy-to-lossless scalability in both l_2 and l_∞ norms, it also provides the highest throughput for both SNR and PAE metrics.

REFERENCES

[1] L. A. C. Lastri, B. Aiazzi and S. Baronti, "Virtually lossless compression of astrophysical images," *EURASIP Journal on Applied Signal Processing*, vol. 15, pp. 2521–2535, 2005.

[2] K. Chen and T. V. Ramabadran, "Near-lossless compression of medical images through entropy-coded dpcm," *IEEE Trans. Med. Imag.*, vol. 13, pp. 538–548, 1994.

[3] S. Yea and W. A. Pearlman, "A wavelet-based two-stage near-lossless coder," *IEEE Trans. Image Process.*, vol. 15, pp. 3488–3500, Nov. 2006.

[4] D. S. Taubman and M. W. Marcellin, *Image Compression Fundamentals, Standards and Practice*. Boston, USA: Kluwer, 2002.

[5] X.Wu, N.Memon, and K. Sayood, "A context-based, adaptive, lossless/nearly-lossless coding scheme for continuous-tone images," *ISO/IEC JTC 1.29.12*, July 1995.

[6] ISO, "ISO/IEC JTC 1/SC 29/WG 1, JPEG LS image coding system," *Working Document N399-WD144495*, July 1996.

[7] X. Wu and P. Bao, "L_∞ constrained high-fidelity image compression via adaptive context modeling," *IEEE Trans. Image Process.*, vol. 9, pp. 536–542, April 2000.

[8] B. Aiazzi, L. Alparone, and S. Baronti, "Context modeling for near-lossless image coding," *IEEE Signal Process. Lett.*, vol. 9, pp. 77–80, March 2002.

[9] G. S. M. J. Weinberger, G. Seroussi, "The loco-i lossless image compression algorithm: principles and standardization into jpeg-ls," *IEEE Trans. Image Process.*, vol. 9, pp. 1309–1324, 2000.

[10] R. Ansari, N. Memon, and E. Ceran, "Near-lossless image compression techniques," *J. Electron. Imag.*, vol. 7, pp. 486–494, 1998.

[11] J. Zhou, X. Wu, and L. Zhang, "l_2 restoration of l_∞-decoded images via soft-decision estimation," *IEEE Trans. Image Process.*, vol. 21, pp. 4797–4807, Dec. 2012.

[12] X. Wu and N. Memon, "Context-based lossless interband compression – extending CALIC," *IEEE Trans. Image Process.*, vol. 9, pp. 994–1001, June 2000.

[13] E. Magli, G. Olmo, and E. Quacchio, "Optimized onboard lossless and near-lossless compression of hyperspectral data using CALIC," *IEEE Geosci. Remote Sens. Lett.*, vol. 1, pp. 21–25, January 2004.

[14] D. Valsesia and E. Magli, "A novel rate control algorithm for onboard predictive coding of multispectral and hyperspectral images," *IEEE Trans. Geosci. Remote Sens.*, vol. 52, pp. 6341–6355, October 2014.

[15] S.-C. Tai, T.-M. Kuo, and N. K. San, "An extension on CCSDS algorithm by ROI capability," *Proceedings of the 2010 Fourth Pacific-Rim Symposium on Image and Video Technology*, pp. 208–213, 2010.

[16] S.-C. Tai, T.-M. Kuo, C.-H. Ho, and T.-W. Liao, "A near-lossless compression method based on CCSDS for satellite images," *International Symposium on Computer, Consumer and Control*, 2012.

[17] F. Garcia-Vilchez and J. Serra-Sagristà, "Extending the CCSDS recommendation for image data compression for remote sensing scenarios," *IEEE Trans. Geosci. Remote Sens.*, vol. 47, pp. 3434–3445, Oct. 2009.

[18] X. Wu, "Near-lossless image compression by combining wavelets and CALIC," *Conf. Rec. of the Thirty-First Asilomar Conference on Signals, Systems amp, Computers 1997*, vol. 2, pp. 1427–1431, November 1997.

[19] A. Said and W. A. Pearlman, "A new fast and efficient image codec based on set partitioning in hierarchical trees," *IEEE Trans. Circuits Syst. Video Technol.*, vol. 6, pp. 243–249, June 1996.

[20] A. Krivoulets, "A method for progressive near-lossless image compression," *Proc. IEEE Int. Conf. Image Processing*, vol. 3, pp. 185–188, 2003.

[21] S. Yea and W. A. Pearlman, "A wavelet-based two-stage near-lossless coder with l_∞-error scalability," *Visual Communications and Image Processing*, vol. SPIE-IS&T 6077, p. 607714, January 2006.

[22] G. Carvajal, B. Penna, and E. Magli, "Unified lossy and near-lossless hyperspectral image compression based on jpeg 2000," *IEEE Geosci. Remote Sens. Lett.*, vol. 5, pp. 593–597, 2008.

[23] C.-W. Chen, T.-C. Lin, S.-H. Chen, and T.-K. Truong, "A near lossless wavelet-based compression scheme for satellite images," *World Congress on Computer Science and Information Engineering*, 2009.

[24] CCSDS, *Image Data Compression, Recommended Standard*. Recommendation for Space Data Systems Standards. CCSDS 122.0-B-1. Blue Book. Issue I. Washington D.C., Nov. 2005.

[25] I. Avcibas, N. Memon, B. Sankur, and K. Sayood, "A progressive lossless/near-lossless image compression algorithm," *IEEE Signal Process. Lett.*, vol. 9, pp. 312–314, October 2002.

[26] I. Avcibas, N. Memon, B. Sankur, and K. Sayood, "A successively refinable lossless image-coding algorithm," *IEEE Trans. Commun.*, vol. 53, pp. 445–452, 2005.

[27] A. Alecu, A. Munteanu, P. Schelkens, J. Cornelis, and S. Dewitte, "On the optimality of embedded deadzone scalar-quantizers for wavelet-based L-infinite-constrained image coding," *IEEE Signal Process. Lett.*, vol. 11, pp. 367–370, March 2004.

[28] J. Zhang, J. Fowler, and G. Liu, "Lossy-to-lossless compression of hyperspectral imagery using three-dimensional TCE and an integer KLT," *IEEE Geosci. Remote Sens. Lett.*, vol. 5, pp. 814–818, October 2008.

[29] I. Blanes and J. Serra-Sagristà, "Cost and scalability improvements to the Karhunen-Loève transform for remote-sensing image coding," *IEEE Trans. Geosci. Remote Sens.*, vol. 7, pp. 2854–2863, July 2010.

[30] Q. Du, N. Ly, and J. E. Fowler, "An operational approach to PCA+JPEG2000 compression of hyperspectral imagery," *IEEE J. Sel. Topics Appl. Earth Observations Remote Sens.*, vol. 7, pp. 2237–2245, June 2014.

[31] A. Krivoulets, "Efficient entropy coding for image compression," IT University of Copenhagen, Tech. Rep., February 2002.

[32] Jet Propulsion Laboratory, NASA, "Airborne Visible InfraRed Imaging Spectrometer website." [Online]. Available: http://aviris.jpl.nasa.gov/

[33] U.S. Geological Survey, "Earth explorer." [Online]. Available: http://earthexplorer.usgs.gov

[34] I. Blanes, E. Magli, and J. Serra-Sagrista, "A tutorial on image compression for optical space imaging systems," *Geoscience and Remote Sensing Magazine, IEEE*, vol. 2, no. 3, pp. 8–26, Sept 2014.

[35] E. Magli, "M-CALIC software." [Online]. Available: http://www.telematica.polito.it/SAS/download/magli/Mcalic.zip

[36] P. W. Hao and Q. Y. Shi, "Matrix factorizations for reversible integer mapping," *IEEE Trans. Signal Process.*, vol. 49, no. 10, pp. 2314–2324, 2001.